Symmetric dynamics in dissipative quantum many-body models

Yi Zheng [1,*] and Shuo Yang [2,3]

[1] *College of Physics and Electronic Engineering, Institute of Solid State Physics, Sichuan Normal University, Chengdu 610068, China*
[2] *State Key Laboratory of Low-Dimensional Quantum Physics and Department of Physics, Tsinghua University, Beijing 100084, China*
[3] *Frontier Science Center for Quantum Information, Beijing 100084, China*

(Received 10 April 2021; revised 15 July 2021; accepted 16 July 2021; published 4 August 2021)

We show symmetric dynamics in dissipative quantum many-body systems. Given some conditions on the Hamiltonian and the jump operators, the time evolution of certain observables can be identical for ferromagnetic and antiferromagnetic interactions in an Ising model with external fields or for repulsive and attractive interactions in a Hubbard model. We present two theorems to determine the existence of such a dynamical symmetry in dissipative quantum systems. The symmetry under the steady state is present independently on the initial state. Further constraint on the initial state leads to a stronger dynamical symmetry in real-time evolutions. We demonstrate the application of our theorems in dissipative Ising and Hubbard models. In addition, for the Fermi-Hubbard model, our results also reveal a connection between spin and charge densities in dissipative dynamics. We validate the discussions with numerical simulations performed using tensor network algorithms.

DOI: 10.1103/PhysRevA.104.023304

I. INTRODUCTION

Recent experiments with ultracold atoms in optical lattices have provided versatile quantum simulations of the bosonic and fermionic Hubbard models [1–5]. This is largely due to the high level of controllability of such systems and the technique of *in situ* measurements with single-site resolution in optical lattices. The interaction between atoms plays an essential role for out-of-equilibrium phenomena. Dramatically, a many-body system with attractive interaction expands instead of shrinks after a quench of the confining potential [1,2]. The expansion velocities turn out to be nearly identical to that with repulsive interactions [2]. At this point, the dynamics can be independent of the sign of the interaction in the Hubbard model. This indicates a dynamical symmetry for closed systems under certain conditions. The existence of such a property is constrained by the presence of certain symmetries in the single-particle Hamiltonian [6]. We show that this discussion is also suitable for the Ising Hamiltonian where the ferromagnetic and antiferromagnetic orders correspond to different signs of the spin-spin interactions.

On the other hand, dissipation occurs in systems coupled to an environment. As a ubiquitous effect in nature, dissipation in quantum systems has received great attention. Dissipative quantum models are at the heart of studying various phenomena, such as parity-time reversal symmetry breaking [7,8], non-Hermitian skin effect [9–11], dissipative binding mechanisms [12,13], and phase transitions of dynamical nonequilibrium steady states [14–38]. Dissipation has been a crucial issue in quantum engineering, since it causes decoherence of the quantum state. It can also be manipulated in the preparation of particular quantum states [39–44]. Understanding the nonequilibrium dynamics is of common interest in a wide range of physical contexts, including ultracold gases [39,40,45–47], trapped ions [48–50], exciton-polariton Bose-Einstein condensates [51], and cavity QED arrays [52–54].

For the dynamics of quantum systems with dissipation, the equation of motion includes coherent parts as well as quantum jumps. Here we present two theorems applicable to dissipative quantum many-body models to determine the existence of the dynamical symmetry. Remarkably, constraints on the quantum jump and the single-particle Hamiltonian induce a symmetry in dynamics for strong-interacting models. We demonstrate the presence of the dynamical symmetry in dissipative Ising and Hubbard models. Furthermore, by applying the theorem to a spin-1/2 Fermi-Hubbard model (FHM) with dissipation, a mapping between spin and charge dynamics is established.

II. DYNAMICAL SYMMETRY

In general, we consider Hamiltonians of the form $\hat{H} = \hat{H}_0 + \xi\hat{H}_{\rm int}$. For the transverse-field Ising model, $\hat{H}_0 = \sum_i \hat{\sigma}_i^x$, and $\hat{H}_{\rm int} = \sum_{\langle i,j\rangle} \hat{\sigma}_i^z\hat{\sigma}_j^z$ is the nearest-neighbor spin interaction, with σ_i^α being the α-Pauli matrix at site i. Here $\xi > 0$ ($\xi < 0$) corresponds to antiferromagnetic (ferromagnetic) interaction. For the Hubbard model, $\hat{H}_0$ includes single-particle hopping terms. The on-site interaction is written either as $\hat{H}_{\rm int} = \sum_i \hat{n}_i(\hat{n}_i - 1)$ for spinless bosons or as $\hat{H}_{\rm int} = \sum_i \hat{n}_{i,\uparrow}\hat{n}_{i,\downarrow}$ for spin-1/2 fermions. Then $\xi > 0$ ($\xi < 0$) corresponds to repulsive (attractive) interaction. The dynamical symmetry here refers to the phenomenon that an observable $\hat{O}$ has the same time-evolution for models with positive (+) and negative (−) ξ, i.e., $\langle\hat{O}(t)\rangle_{+\xi} = \pm\langle\hat{O}(t)\rangle_{-\xi}$.

Since a pure state evolves as $|\psi(t)\rangle = e^{-i(\hat{H}_0+\xi\hat{H}_{\rm int})t}|\psi_0\rangle$, the combination of time reversal and an operation (which flips the sign of $\hat{H}_0$) leads to the dynamics of an effective Hamiltonian $\hat{H}_0 - \xi\hat{H}_{\rm int}$. Let us take the transverse-field Ising model $\hat{H} = (h_x/2)\sum_i \hat{\sigma}_i^x + (J/4)\sum_{\langle i,j\rangle} \hat{\sigma}_i^z\hat{\sigma}_j^z$ as an example.

*zhengyireal@126.com

 ©2021 American Physical Society

The physics is unchanged under a π rotation around the z axis in spin space ($\hat{W}^{-1}\hat{\sigma}_x\hat{W} = -\hat{\sigma}_x$ and $\hat{W}^{-1}\hat{\sigma}_y\hat{W} = -\hat{\sigma}_y$ with $\hat{W} = e^{\pm\frac{i}{2}\pi\hat{\sigma}_z}$). By applying time reversal followed by this rotation, we can map the evolution operator $e^{-i\hat{H}t}$ of an antiferromagnetic model to that of a ferromagnetic model. Thus, as long as the initial state satisfies $(\hat{R}\hat{W})^{-1}|\psi_0\rangle = e^{i\phi}|\psi_0\rangle$, with $\hat{R}$ being the time-reversal operator ($\hat{R}^{-1}i\hat{R} = -i$) and ϕ an arbitrary phase, we have $\langle\hat{O}(t)\rangle_{+J} = \langle\hat{O}(t)\rangle_{-J}$ for $\hat{O} = \hat{\sigma}_z, \hat{\sigma}_y$ and $\langle\hat{O}(t)\rangle_{+J} = -\langle\hat{O}(t)\rangle_{-J}$ for $\hat{O} = \hat{\sigma}_x$, with $+$ or $-$ in the subscripts indicating the sign of J.

The dynamics of dissipative quantum systems can be described by means of a master equation, which is obtained by tracing over the degree of freedom of the environment [55–57]. For Markovian systems, the Lindblad master equation constitutes the most general form, which is given by

$$\frac{d}{dt}\hat{\rho} = -i[\hat{H},\hat{\rho}] + \sum_{\mu}\gamma\left(\hat{L}_\mu\hat{\rho}\hat{L}_\mu^\dagger - \frac{1}{2}\{\hat{L}_\mu^\dagger\hat{L}_\mu,\hat{\rho}\}\right). \quad (1)$$

Here $\hat{\rho}$ is the reduced density matrix of the system, $\hat{H}$ is the system Hamiltonian, and $\hat{L}_\mu$ are the Lindblad operators, which describe the dissipation. $[\cdots]$ and $\{\cdots\}$ denote commutator and anticommutator. γ is a positive constant quantifying the dissipation rate. We have set $\hbar = 1$ for convenience. The first term on the right-hand side of Eq. (1) describes the unitary evolution, as in the case of Liouville-von Neumann equation. The second term is the Lindbladian describing the nonunitary quantum jumps. The dissipative dynamics of Eq. (1) often leads to a nonequilibrium steady state $\hat{\rho}_{\rm ss} = \lim_{t\to\infty}\hat{\rho}(t)$ satisfying $\frac{d}{dt}\hat{\rho}_{\rm ss} = 0$. Here we assume that the stationary state is unique, which is indeed the case under quite general assumptions [58–60]. In contrast to closed quantum systems, the existence of the dynamical symmetry in dissipative models requires us to pose conditions on the jump operators $\hat{L}_\mu$. We present our findings in the form of two theorems.

Theorem 1. For a dissipative quantum model with a Hamiltonian $\hat{H} = \hat{H}_0 + \xi\hat{H}_{\rm int}$ and jump operators $\hat{L}_\mu$, we consider the measurement of an observable $\hat{O}$ under steady state $\hat{\rho}_{\rm ss}$. We have $\langle\hat{O}\rangle_{{\rm ss},+\xi} = \pm\langle\hat{O}\rangle_{{\rm ss},-\xi}$ upon finding an antiunitary operator $\hat{S}$ that satisfies the following conditions: (i) $\{\hat{S},\hat{H}_0\} = 0$ and $[\hat{S},\hat{H}_{\rm int}] = 0$, (ii) $\hat{S}^{-1}\hat{L}_\mu\hat{S} = e^{i\phi}\hat{L}_\mu$ with ϕ an arbitrary phase, and (iii) $\hat{S}^{-1}\hat{O}\hat{S} = \pm\hat{O}$. Here the expectation value $\langle\hat{O}\rangle_{{\rm ss},\pm\xi}$ corresponds to the steady state with $\pm\xi$.

Proof of Theorem 1. Equation (1) can be written as $d\hat{\rho}/dt = \hat{\mathcal{L}}[\hat{\rho}]$ with $\hat{\mathcal{L}}$ the Liouvillian superoperator. Straightforwardly, with conditions (i) and (ii), we have $\hat{S}^{-1}\hat{\mathcal{L}}[\hat{\rho}_{\rm ss}]_{+\xi}\hat{S} = \hat{\mathcal{L}}[\hat{S}^{-1}\hat{\rho}_{ss}\hat{S}]_{-\xi} = 0$, where $\hat{\rho}_{\rm ss}$ is the steady state corresponding to $\hat{\mathcal{L}}(+\xi)$. Thus $\hat{S}^{-1}\hat{\rho}_{\rm ss}\hat{S}$ is the steady state for $\hat{\mathcal{L}}(-\xi)$. If we further have condition (iii), we can conclude that

$$\langle\hat{O}\rangle_{ss,+\xi} = {\rm Tr}(\hat{S}^{-1}\hat{\rho}_{ss}\hat{S}\hat{S}^{-1}\hat{O}\hat{S}) = \pm\langle\hat{O}\rangle_{ss,-\xi}. \quad (2)$$

In practice, it is convenient to express $\hat{S} = \hat{R}\hat{W}$ with $\hat{R}$ the antiunitary time-reversal operator and $\hat{W}$ a unitary operator. This is based on the fact that a time-reversal operation is equivalent to inverting the sign of $\hat{H}$. Then we need to find $\hat{W}$ that may invert the sign of $\hat{H}_0$. Condition (ii) is easily satisfied when considering atom gain (loss) in the case of a Hubbard model or spin flip in the case of spin models. This theorem can be taken as an advantage in analyzing the steady-state phase diagram.

Theorem 2. We consider the real time-evolution starting from an initial state ρ_0. Upon finding an antiunitary operator $\hat{S}$ that satisfies conditions (i)–(iii) in *Theorem 1* as well as (iv) $[\hat{S},\hat{\rho}_0] = 0$, we have $\langle\hat{O}(t)\rangle_{+\xi} = \pm\langle\hat{O}(t)\rangle_{-\xi}$ with the $\pm$ sign in accordance with that in (iii).

Proof of Theorem 2. We utilize the so-called Choi's isomorphism, which can be intuitively understood by the mapping $|\psi\rangle\langle\phi| \leftrightarrow |\psi\rangle\otimes|\phi\rangle$ [61,62]. The insight is to vectorize (reshape) the density matrix $\hat{\rho}$ into a super-ket state $|\rho\rangle_\#$ and rewrite Eq. (1) as $|\dot{\rho}\rangle_\# = \hat{\mathcal{L}}_\#|\rho\rangle_\#$. Here (see the Appendix for details)

$$\hat{\mathcal{L}}_\# = -i(\hat{H}\otimes\hat{I} - \hat{I}\otimes\hat{H}^T) + \sum_\mu\left(\hat{L}_\mu\otimes\hat{L}_\mu^* - \frac{1}{2}\hat{L}_\mu^\dagger\hat{L}_\mu\otimes\hat{I} - \frac{1}{2}\hat{I}\otimes\hat{L}_\mu^T\hat{L}_\mu^*\right) \quad (3)$$

is the vectorized Liouvillian superoperator [62]. Operators on the two sides of $\otimes$, respectively, act on the ket and the bra of $\hat{\rho}$. $\hat{I}$ is a $d\times d$ identity matrix with $d = \dim(\hat{H})$. In addition, we have the mapping

$${\rm Tr}(\hat{\rho}\hat{O}) \leftrightarrow_\# \langle O|\rho\rangle_\#, \quad \hat{S}^{-1}\hat{O}\hat{S} \leftrightarrow \hat{\mathbb{S}}^{-1}|O\rangle_\#, \quad (4)$$

with $|O\rangle_\#$ the vectorized observation operator and $\hat{\mathbb{S}}^{-1} \equiv (\hat{S}^{-1}\otimes\hat{S}^T)$. Now with conditions (iii) and (iv), the expectation value of $\hat{O}$ is given by

$$\begin{aligned}\langle\hat{O}(t)\rangle &= {}_\#\langle O|e^{\hat{\mathcal{L}}_\# t}|\rho_0\rangle_\# =_\# \langle O|\hat{\mathbb{S}}\hat{\mathbb{S}}^{-1}e^{\hat{\mathcal{L}}_\# t}\hat{\mathbb{S}}\hat{\mathbb{S}}^{-1}|\rho_0\rangle_\# \\ &= \pm_\#\langle\mathcal{O}|e^{\hat{\mathbb{S}}^{-1}\hat{\mathcal{L}}_\#\hat{\mathbb{S}}\,t}|\rho_0\rangle_\#. \end{aligned} \quad (5)$$

From Eq. (3), we can straightforwardly verify that $\hat{\mathbb{S}}^{-1}\hat{\mathcal{L}}_\#(+\xi)\hat{\mathbb{S}} = \hat{\mathcal{L}}_\#(-\xi)$ under conditions (i) and (ii) (see the Appendix). This leads to $\langle\hat{O}(t)\rangle_{+\xi} = \pm\langle\hat{O}(t)\rangle_{-\xi}$ from Eq. (5).

This theorem imposes a restriction on the initial density matrix and leads to a stronger constraint on the dynamics induced by interactions. As will be demonstrated in the following examples, condition (iv) can be easily fulfilled, especially for pure states such as a spin ordered state or a Fock state. In fact, we can always choose an eigenstate of $H_{\rm int}$ as the initial state which satisfies condition (iv). This indicates that *theorem 1* can be inferred from *theorem 2*. We mention that our theorems are applicable to spin models with spin-1/2 and larger spins. They are also suitable for tight-binding models with both fermions and bosons. In addition, the theorems have no restriction on the form of interactions, more complicated cases are also considerable, such as three-body interactions [63–66] or long-range interactions [67–69] in the Hubbard model.

III. NUMERICAL METHOD

There have been numerical efforts in simulating dissipative quantum many-body systems [70–73]. To perform time evolutions, we take the recent proposed tensor network (TN) method which is based on the TN representation of a quantum state/operator [62]. The main idea is to map an operator (such as projected entangled-pair operators) to a TN state (such as a projected entangled-pair state (PEPS) [74,75]) according to Choi's isomorphism. This is done by binding the two physical

indices into a single one through $(i, j) \to j \cdot d + i$, with i and j the row and column indices of the operator in its matrix form. Thus the traditional TN algorithms can be applied. The infinite-PEPS (iPEPS) algorithm has been demonstrated to be reliable in simulating the steady state of two-dimensional (2D) square lattice systems in the thermodynamic limit [62]. Here we use the projected entangled-simplex operator TN [76] as a representation of the density matrix and apply the simple update algorithm [77,78]. For infinite 2D systems, the TN is translationally invariant and we take a 2×2 unit cell. This method is efficient and stable in real-time simulations with bond dimensions $D = 6$ for the spin-1/2 model and $D = 4$ for the Bose-Hubbard model. A time step $\delta t \sim 0.01$ is sufficient in our simulations. We apply the corner transfer matrix method (CTM) [79] to contract the TN for the expectation value of an observable. Convergence of the results have been verified with the truncated bond dimension $\chi = 10$ in CTM.

IV. DISSIPATIVE ISING MODEL

Let us now consider a dissipative Ising model on an infinite 2D square lattice as an example of a system satisfying our theorems. We focus on a spin-1/2 quantum system with $\hat{L}_\mu = \hat{\sigma}_\mu^-$, where $\hat{\sigma}_\mu^- = \hat{\sigma}_\mu^x - i\hat{\sigma}_\mu^y$ is the spin lowering operator and μ is the site index. We set $\gamma = 0.1$ for the decay rate. The dynamics is governed by the master equation (1) with the Hamiltonian given by

$$\hat{H} = \frac{h_x}{2}\sum_i \hat{\sigma}_i^x + \frac{h_z}{2}\sum_i \hat{\sigma}_i^z + \frac{J}{4}\sum_{\langle i,j\rangle} \hat{\sigma}_i^z\hat{\sigma}_j^z. \tag{6}$$

Here J is the interaction strength and h_x (h_z) is the strength of the transverse (longitudinal) field. This model has received theoretical and experimental interest due to its connection to the systems of driven-dissipative Rydberg gases [24,70,80–82]. The steady states are expected to exhibit a first-order phase transition akin to the liquid-gas transition [70,82]. We take the up spins as particles and measure its density $n_\uparrow = \sum_{i=1}^N \langle(\hat{1} + \hat{\sigma}_i^z)\rangle/(2N)$ (with i runs over all lattice sites).

We first consider the case of $h_z = 0$ and hence $\hat{H}_0 = (h_x/2)\sum_i \hat{\sigma}_i^x$. We find $\hat{S} = \hat{R}(\otimes_i \hat{\sigma}_i^z)$, which commutes with the spin-spin interaction part, such that $\{\hat{S}, \hat{\sigma}_i^x\} = 0$, $[\hat{S}, (\hat{1} + \hat{\sigma}_i^z)] = 0$ and $\{\hat{S}, \hat{\sigma}^-\} = 0$. One immediately sees that the measurements of $n_\uparrow$ under steady states are the same for ferromagnetic ($J < 0$) and antiferromagnetic ($J > 0$) interactions. As a demonstration, we set a random density matrix $\hat{\rho}_r$ as the initial state and perform simulations with $J = \pm 5\gamma$, $h_x = 5\gamma$, and 8γ. Results are shown in Figs. 1(a1) and 1(a2). In long-time evolutions, the densities of up spins lead to the same value for both $J = 5\gamma$ and -5γ. Obviously, $\hat{\rho}_0 = \hat{\rho}_r$ does not commute with $\hat{S}$ and hence there is no symmetry in real-time evolutions. On the other hand, condition (iv) is satisfied if we assume the initial state to be of the form $\hat{\rho}_0 = \sum_n P_n|\phi_n\rangle\langle\phi_n|$, where $|\phi_n\rangle = |s_1, \cdots, s_N\rangle_n$ and $|s_i\rangle$ is an eigenstate of $\hat{\sigma}^z$. As an example, we choose $\hat{\rho}_0 = |\downarrow\cdots\downarrow\rangle\langle\downarrow\cdots\downarrow|$. The spin-up densities $n_\uparrow$ follow exactly the same evolution as can be seen from Figs. 1(b1) and 1(b2) with $J = -5\gamma$ and $J = 5\gamma$.

In the presence of a longitudinal field $(h_z/2)\sum \hat{\sigma}_i^z$, we include this term in the spin-interaction part $\hat{H}_{\rm int}$ instead of

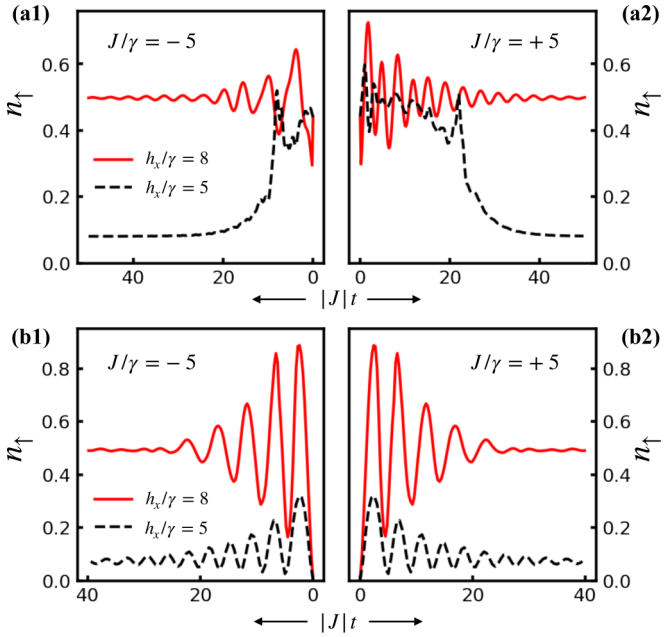

FIG. 1. Time evolution of spin-up density $n_\uparrow$ in the dissipative transverse-field Ising model. (a1), (a2) Real-time evolutions with ferromagnetic interaction ($J/\gamma = -5$) and antiferromagnetic interaction ($J/\gamma = 5$). The upper and lower curves correspond to $h_x/\gamma = 8$ and 5, respectively. The evolutions start from a random mixed state. There is no symmetry in real-time evolutions. However, on approaching steady states, spin-up densities become symmetric between $J/\gamma = -5$ and $J/\gamma = +5$. (b1), (b2) The same as (a1), (a2) but with the initial state set to be a polarized state with all spins pointing down. The dynamical symmetry is satisfied.

$\hat{H}_0 = (h_x/2)\sum \hat{\sigma}_i^z$. By this choice, our theorem still applies with the same antiunitary operator $\hat{S}$ as in the case of $h_z = 0$. Now the conclusion is about the symmetry between $(+J, \pm h_z)$ and $(-J, \mp h_z)$, i.e., between antiferromagnetic interactions with positive (negative) longitudinal field and ferromagnetic interactions with negative (positive) longitudinal field. As shown in Fig. 2(a) with $h_x = 6.5\gamma$, $\pm h_z = \pm 0.5\gamma$, and $\pm J = \pm 5\gamma$, the time dependence of $n_\uparrow$ for $(+J, +h_z)$ differs from that for $(-J, +h_z)$, but is equivalent to the case of $(-J, -h_z)$.

Symmetric behaviors also appear in the steady-state phase diagram. In Fig. 2(b), we show the spin-up density $n_\uparrow$ (under steady states) as a function of h_x. The sudden jump of $n_\uparrow$ indicates a first-order transition from a lattice gas phase with low density of up spins to a lattice liquid phase characterized by nearly half-filling of up spins and vanishing compressibility $(-\partial n_\uparrow/\partial h_x)$ [35,70]. For $J = 5\gamma$ and $h_z = 0$, the solid curve with the transition point at $h_x \sim 6\gamma$ is in good agreement with the results from both the variational method with correlated ansatz [70] and the real-time simple update with iPEPS [62]. The transition point shifts leftward (rightward) with positive (negative) h_z. We observe that the $n_\uparrow$-h_x relations with $(J, h_z)/\gamma = (5, 0)$, (5,0.5), and $(5, -0.5)$ reproduce those with $(J, h_z)/\gamma = (-5, 0)$, $(-5, -0.5)$, and $(-5, 0.5)$, respectively. We complement our demonstration with the h_x-h_z phase diagram, as depicted in Fig. 2(c) for $J = +5\gamma$ and Fig. 2(d) for $J = -5\gamma$. One can clearly see that the diagrams for antiferromagnetic and ferromagnetic

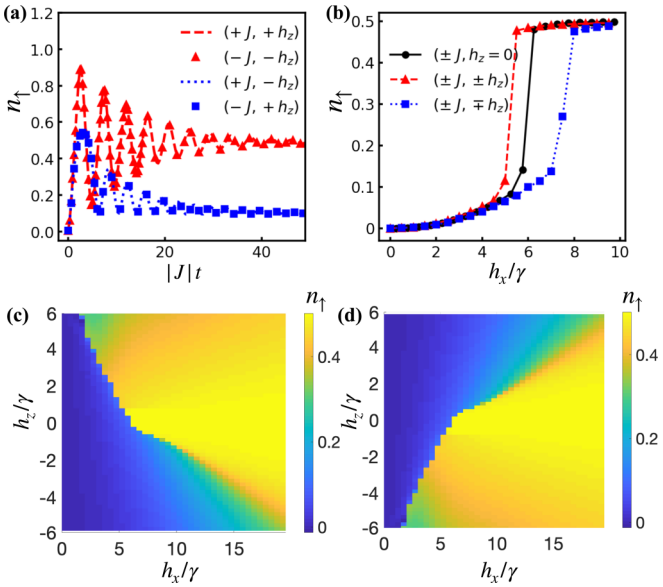

FIG. 2. (a) Time dependence of spin-up density $n_\uparrow$ in the dissipative Ising model with transverse field ($h_x/\gamma = 6.5$) and longitudinal field. $n_\uparrow(t)$ obtained with parameters $(+J, +h_z)$ (red dashed line) differs from that for $(-J, +h_z)$ (blue square) but it agrees with the data of $(-J, -h_z)$ (red triangle). (b) Spin-up density $n_\uparrow$ under steady state as a function of h_x. Steady states for $(+J, \pm h_z)$ and $(-J, \mp h_z)$ share the same $n_\uparrow$. We take $\pm J = \pm 5\gamma$ and $\pm h_z = \pm 0.5\gamma$ in all plots. (c), (d) The steady-state phase diagram spanned by h_x and h_z. The two diagrams in (c) and (d) are for antiferromagnetic $(+J)$ and ferromagnetic $(-J)$ models. They are symmetric about $h_z = 0$.

interacting models are symmetric about the $(h_z = 0)$ axis. The symmetry of phase diagrams is due to the dissipative nature of the system, which is remarkably different from the situation in closed quantum systems. Note that in nondissipative Ising models with a small transverse field, the antiferromagnetic and ferromagnetic interactions correspond to distinct phases that are characterized by $n_\uparrow = 1/2$ and 1, respectively.

V. DISSIPATIVE HUBBARD MODEL

We proceed by considering a dissipative Hubbard model. We first take the Bose-Hubbard model with two-body inelastic atom loss as a demonstration. This consideration is motivated by the recent experimental realization with ultracold gases in an optical lattice [83]. The experiment in Ref. [83] implemented a slow ramp-down of lattice depth starting from a Mott insulator to observe the crossover to superfluid state. The atom number per site can be measured through fluorescence detection. Here we consider the quench dynamics in a 2D square lattice and show that the time evolutions of the average density are symmetric between repulsive and attractive interactions.

The two-body dissipation can be engineered through a single photon photoassociation process for ultracold lattice gases [83], which leads to the jump operator of the form $\hat{L}_\mu = \sqrt{\gamma}\hat{b}_\mu\hat{b}_\mu$. The Hamiltonian is given by

$$\hat{H} = -\sum_{\langle j,l\rangle} \hat{b}_j^\dagger \hat{b}_l + \frac{U}{2}\sum_j \hat{n}_j(\hat{n}_j - 1), \tag{7}$$

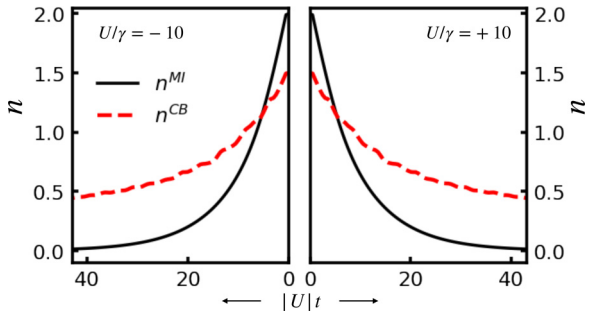

FIG. 3. Decay of the average density n in the Bose-Hubbard model with two-body atom loss. The evolutions start from a double-filled MI or a (2,1)-filled CB state. The time-dependent densities are symmetric between the attractive (left panel) and repulsive (right panel) models.

with $\hat{b}_j$ ($\hat{b}_j^\dagger$) the bosonic annihilation (creation) operator and $\hat{n}_j = \hat{b}_j^\dagger\hat{b}_j$. The dynamical symmetry corresponds to the unitary operator $\hat{W}$ given by $\hat{W}^{-1}\hat{b}_j\hat{W} = (-1)^j\hat{b}_j$. Then $\hat{S} = \hat{R}\hat{W}$ commutes with the interaction term and anticommutes with $\hat{H}_0 = -\sum_{\langle j,l\rangle}\hat{b}_j^\dagger\hat{b}_l$. Explicitly, we present $\hat{W} = \otimes_j \exp[i\frac{\pi}{2}\hat{n}_j + (-1)^j i\frac{\pi}{2}\hat{n}_j]$ that meets the requirements. As a result, the relation $\hat{S}^{-1}\hat{L}_\mu S = e^{i\phi}\hat{L}_\mu$ is always fulfilled for on-site dissipations consisting of $\hat{b}_j$ and $\hat{b}_j^\dagger$ (e.g., $\hat{L}_\mu = \hat{b}_j$, $\hat{L}_\mu = \hat{b}_j\hat{b}_j$ or $\hat{L}_\mu = \hat{n}_{j,\downarrow}^\dagger$). In general, we take the initial state as $\hat{\rho}_0 = \sum_m P_m|\phi_m\rangle\langle\phi_m|$ with $|\phi_m\rangle = |n_1, \cdots, n_N\rangle_m$, and the physical operator as $\hat{O} = (1/N)\sum_{j=1}^N \hat{n}_j$. It is straightforward to verify that $\hat{S}$ commutes with $\hat{\rho}_0$ and $\hat{O}$. Thus, conditions (i)–(iv) are all satisfied and the dynamical symmetry $\langle\hat{O}(t)\rangle_{+U} = \langle\hat{O}(t)\rangle_{-U}$ is guaranteed. We show results of numerical simulations in Fig. 3 with $\gamma = 0.5$, $U = \pm 5$. We measure the time dependence of the average density. The evolutions start from a double-filled Mott insulator (MI) (black lines) and a checkerboard state with filling factors $n_A = 2$ and $n_B = 1$ on neighboring sites (red dashed lines). Both cases lead to identical density decays in attractive and repulsive interacting systems. Note that the analysis can be directly extended to other realizable configurations, including the Harper-Hofstadter Hamiltonian [5] and the Aubre-André model [3].

Considering the fermionic case can lead to more interesting results. We turn to the dissipative FHM with the Hamiltonian given by

$$H_{\rm FHM} = -\sum_{\langle i,j\rangle,\sigma} \hat{c}_{i,\sigma}^\dagger\hat{c}_{j,\sigma} + U\sum_i\left(\hat{n}_{i\uparrow} - \frac{1}{2}\right)\left(\hat{n}_{i\downarrow} - \frac{1}{2}\right), \tag{8}$$

where $\hat{n}_{i,\sigma} = c_{i,\sigma}^\dagger c_{i,\sigma}$ and $c_{i,\sigma}$ ($c_{i,\sigma}^\dagger$) is the fermionic annihilation (creation) operator acting on site i with spin $\sigma \in \{\uparrow, \downarrow\}$. We have set the interaction term in a particle-hole symmetric form. The above analysis can also be applied here by simply appending a spin dependance to the operators. Analogously, the unitary operator $\hat{W}$ is defined by $\hat{W}^{-1}\hat{c}_{j,\sigma}\hat{W} = (-1)^j\hat{c}_{j,\sigma}$ and the dynamical symmetry appears for $\hat{O} = \hat{n}_{i,\sigma}$.

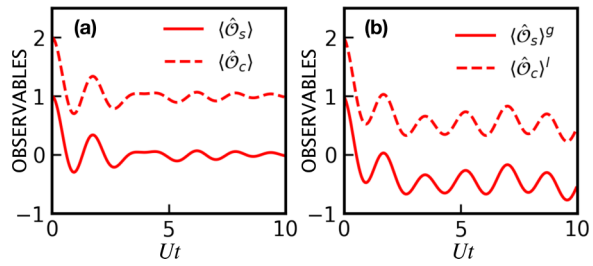

FIG. 4. Time evolution of $\langle \hat{O}_s \rangle$ starting from $|\psi_{\rm SDW}\rangle$ and time evolution of $\langle \hat{O}_c \rangle$ starting from $|\psi_{\rm CDW}\rangle$. (a) The dissipation in the FHM is given by $\hat{L}_\mu = \hat{n}^\dagger_{i,\downarrow}$ (dashed and solid lines). (b) The dissipations are $\hat{L}_\mu = \hat{c}_{i,\downarrow}$ (dashed line) and $\hat{L}_\mu = \hat{c}^\dagger_{i,\downarrow}$ (solid line).

Furthermore, it is of natural interest to study the spin and charge dynamics of the FHM. Recently, the measurements of spin and charge transport have been performed, respectively, by the MIT group and the Princeton group [84,85]. For the two kinds of dynamics, we can take a spin density wave $|\psi_{\rm SDW}\rangle = \prod_s \hat{c}^\dagger_{2s+1,\uparrow}\hat{c}^\dagger_{2s,\downarrow}|0\rangle$ or a charge density wave $|\psi_{\rm CDW}\rangle = \prod_s \hat{c}^\dagger_{2s+1,\uparrow}\hat{c}^\dagger_{2s+1,\downarrow}|0\rangle$ as the initial state. The corresponding observable operators are $\hat{O}_s = \hat{n}_{i,\uparrow} - \hat{n}_{i,\downarrow}$ and $\hat{O}_c = \hat{n}_{i,\uparrow} + \hat{n}_{i,\downarrow}$. These two dynamics can be equivalent under certain conditions for closed systems [86]. We show that this is also the case with dissipations of the form $\hat{L}_\mu = \hat{n}^\dagger_{j,\downarrow}$. Such a Lindblad operator refers to the effect of incoherent light scattering where the dominant process is to scatter an atom into higher bands followed by a spontaneous emission [87]. Upon a particle-hole transformation defined as $\hat{P}^{-1}\hat{c}_{i,\downarrow}\hat{P} = (-1)^i\hat{c}^\dagger_{i,\downarrow}$, $\hat{P}^{-1}\hat{c}^\dagger_{i,\downarrow}\hat{P} = (-1)^i\hat{c}_{i,\downarrow}$ (the operators for spin-$\uparrow$ are left invariant), we have $\hat{P}^{-1}\hat{O}_c\hat{P} = \hat{O}_s + 1$ and $\hat{P}^{-1}\hat{\rho}_c\hat{P} = \hat{\rho}_s$, where $\hat{\rho}_c \equiv |\psi_{\rm CDW}\rangle\langle\psi_{\rm CDW}|$ and $\hat{\rho}_s \equiv |\psi_{\rm SDW}\rangle\langle\psi_{\rm SDW}|$. It is straightforward to verify that $\hat{\mathcal{P}}^{-1}\hat{\mathcal{L}}_\#(+U)\hat{\mathcal{P}} = \hat{\mathcal{L}}_\#(-U)$ with $\hat{\mathcal{L}}_\#(\pm U)$ the Liouvillian superoperator (3) with interaction strength $\pm U$ and $\hat{\mathcal{P}}^{-1} \equiv (\hat{P}^{-1} \otimes \hat{P}^T)$. Following Eq. (5) with $\hat{\mathbb{S}}$ replaced by $\hat{\mathcal{P}}$, we conclude that the time evolution of $\langle \hat{O}_c \rangle_{+U}$ starting from $\hat{\rho}_c$ is exactly equivalent to the time evolution of $\langle \hat{O}_s + 1\rangle_{-U}$ starting from $\hat{\rho}_s$. We further apply the result of dynamical symmetry and relate the time evolutions for repulsive and attractive interactions. Then we obtain $\langle \hat{O}_c(t)\rangle_{{\rm CDW},+U} = \langle \hat{O}_s(t) + 1\rangle_{{\rm SDW},+U}$, which maps the measurement of charge density to that of spin density.

However, in the situation of atom loss (gain), e.g., $\hat{L}_\mu = \hat{c}_{i,\downarrow}$ ($\hat{c}^\dagger_{i,\downarrow}$), the conclusion is altered since now $\hat{\mathcal{P}}^{-1}\hat{\mathcal{L}}_\#(+U, \text{loss})\hat{\mathcal{P}} = \hat{\mathcal{L}}_\#(-U, \text{gain})$. Consequently, $\langle \hat{O}_c(t)\rangle_{+U}$ starting from $\hat{\rho}_c$ in the FHM with atom loss (gain) is exactly equivalent to $\langle \hat{O}_s(t) + 1\rangle_{+U}$ starting from $\hat{\rho}_s$ with atom gain (loss). This proposition provides a linking between atom gain and atom loss in the FHM. In Fig. 4, we show a numerical verification (through exact diagonalization method) of the above relations in one-dimensional dissipative FHM with $\gamma = 0.5$, $U = 1$ and lattice size $L = 6$. For simplicity, we prepare the model initially in $|\psi_{\rm SDW}\rangle$ and $|\psi_{\rm CDW}\rangle$, respectively, followed by the measurements of spin density $\hat{O}_s = \hat{n}_{L/2,\uparrow} - \hat{n}_{L/2,\downarrow}$ (solid lines) and charge density $\hat{O}_c = \hat{n}_{L/2,\uparrow} + \hat{n}_{L/2,\downarrow}$ (dashed lines). In Fig. 4(a), we have set $\hat{L}_\mu = \hat{n}_{i,\downarrow}$ and the relation $\langle \hat{O}_c(t)\rangle_{\rm CDW} = \langle \hat{O}_s(t) + 1\rangle_{\rm SDW}$ holds. Whereas in Fig. 4(b) we set $\hat{L}_\mu = \hat{c}^\dagger_{i,\downarrow}$ and $\hat{L}_\mu = \hat{c}_{i,\downarrow}$, respectively, for spin and charge dynamics. We observe $\langle \hat{O}_c(t)\rangle^{\rm loss}_{\rm CDW} = \langle \hat{O}_s(t) + 1\rangle^{\rm gain}_{\rm SDW}$ as expected.

VI. SUMMARY AND DISCUSSION

In summary, we have provided two theorems to characterize the situations in which a dynamical symmetry may appear in dissipative quantum many-body systems. Applications to Ising and Hubbard models suggest that the symmetric behaviors in the time evolutions is connected to the intrinsic features of the dissipation system. In contrast to closed systems, the symmetry for steady states is valid without the constraint on initial states. This can be propitious to the symmetry analysis for steady-state phases. The discussion on dissipative FHM also reveals a connection between spin and charge dynamics, as well as a connection between atom loss and gain. Our theorems and propositions are rigorous and the results can be readily verified by experiments. As dissipation is ubiquitous in nature, our findings may also have applications in future experiments with dissipative quantum many-body systems, such as in the study of lattice gases, Rydberg polaritons, optical cavities, as well as solid-state materials.

It is worth noting that for non-Markovian systems, understanding the dynamics remains a challenging task due to the memory effects characterized by the exchange of information between the system and the reservoir [88,89]. In Markovian systems, the decay rate γ is a positive constant. By writing this decay rate as $\gamma_\mu(t)$ (which may oscillate over time and take negative values), Eq. (1) can be referred to as a time-local non-Markovian master equation, which describes the dynamics of some particular open systems [90,91]. In this case, we obtain $|\rho(t)\rangle_\# = e^{\int \hat{\mathcal{L}}_\#(t)dt}|\rho_0\rangle_\#$ and Eq. (5) can be rewritten as

$$\begin{aligned}\langle \hat{O}(t)\rangle &= {}_\#\langle O|\hat{\mathbb{S}}\hat{\mathbb{S}}^{-1}e^{\int \hat{L}_\#(t)dt}\hat{\mathbb{S}}\hat{\mathbb{S}}^{-1}|\rho_0\rangle_\# \\ &= \pm{}_\#\langle \mathcal{O}|e^{\int \hat{\mathbb{S}}^{-1}\hat{\mathcal{L}}_\#(t)\hat{\mathbb{S}}\,dt}|\rho_0\rangle_\#. \end{aligned} \tag{9}$$

The time dependance of $\gamma_\mu(t)$ has no effect on verifying the relation $\hat{\mathbb{S}}^{-1}\hat{\mathcal{L}}_\#(+\xi)\hat{\mathbb{S}} = \hat{\mathcal{L}}_\#(-\xi)$. Thus, our results may also be applicable in such a situation. Investigating the dynamical symmetry in concrete models of non-Markovian systems are of our further interest.

ACKNOWLEDGMENTS

This work is supported by the National Key R&D Program of China (Grant No. 2018YFA0306504), NSFC (Grant No. 11804181), and the China Postdoctoral Science Foundation (Grant No. 2019M650025). S.Y. acknowledges support from the National Thousand Young Talents Program and Tsinghua University Initiative Scientific Research Program.

APPENDIX: GRAPHICAL REPRESENTATIONS OF THE FORMALISM

To have an intuitional understanding of Choi's isomorphism [61,62], we introduce a graphical representation as illustrated in Fig. 5. Now Eq. (1) is represented by Fig. 5(a). The density matrix and operators are shown in their matrix forms. The two open legs are physical indices indicating the row and column of those matrices. Connecting two legs

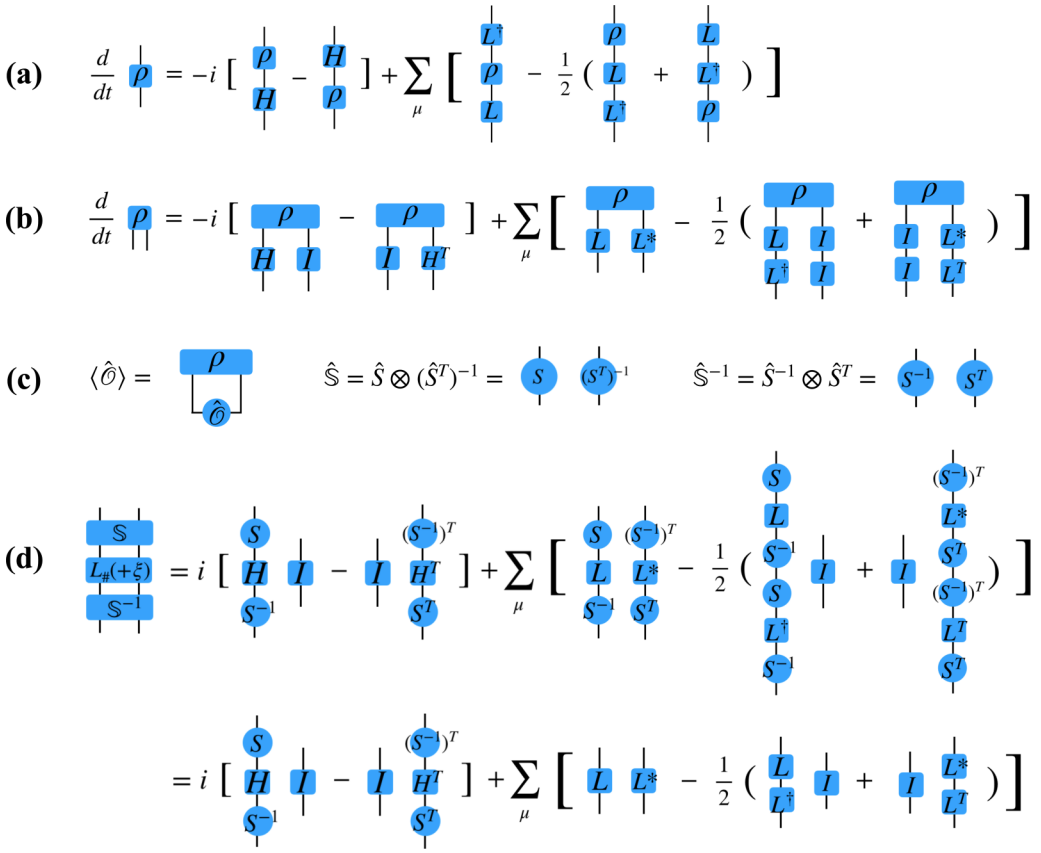

FIG. 5. Graphical representations of (a) the Lindblad master equation (1), (b) the equation for vectorized density matrix [Eq. (A1)], and (c) expectation value of an observable $\hat{O}$ as well as the superoperators $\hat{\mathbb{S}} = \hat{S} \otimes (\hat{S}^T)^{-1}$ and $\hat{\mathbb{S}}^{-1} = \hat{S}^{-1} \otimes \hat{S}^T$. (d) Operation of $\hat{\mathbb{S}}$ acting on the Liouvillian superoperator $\hat{\mathcal{L}}_\#$ with graphical representations given in (a)–(c).

means matrixmultiplication (or tensor contraction for rank-2 tensors). According to the isomorphism, we can rewrite Eq. (1) as

$$\frac{d}{dt}|\rho\rangle_\# = \hat{\mathcal{L}}_\#|\rho\rangle_\# \tag{A1}$$

and hence $|\rho(t)\rangle_\# = e^{\hat{\mathcal{L}}_\# t}|\rho_0\rangle_\#$. Here $|\rho\rangle_\#$ is the vectorized density matrix and $\hat{\mathcal{L}}_\#$ is the Liouvillian superoperator given by Eq. (3). To vectorize the density matrix and obtain Eq. (A1), we simply bend the upper leg down to form the Equation in Fig. 5(b). Note that this notation is widely adopted in the TN language [62,74,75]. We can bind the two downward legs into a row index and treat this density matrix as a ket state $|\rho\rangle_\#$. Thus Fig. 5(b) yields Eq. (A1). In addition, the expectation of $\hat{O}$, the operators $\hat{\mathbb{S}}$ and $\hat{\mathbb{S}}^{-1}$ are graphically shown in Fig. 5(c).

Now conditions (iii) and (iv) are interpreted as $\hat{S}^{-1}\hat{O}\hat{S} = \hat{\mathbb{S}}^\dagger|O\rangle_\# = \pm|O\rangle_\#$ and $\hat{S}^{-1}\hat{\rho}_0\hat{S} = \hat{\mathbb{S}}^{-1}|\rho_0\rangle_\# = |\rho_0\rangle_\#$, respectively. If we have such an $\hat{S}$,

$$\begin{aligned}\langle\hat{O}(t)\rangle &= \langle O|\rho\rangle_\# =_\# \langle O|e^{\hat{\mathcal{L}}_\# t}|\rho_0\rangle_\# \\ &= {}_\#\langle O|\hat{\mathbb{S}}\hat{\mathbb{S}}^{-1}e^{\hat{\mathcal{L}}_\# t}\hat{\mathbb{S}}\hat{\mathbb{S}}^{-1}|\rho_0\rangle_\# \\ &= \pm{}_\#\langle O|e^{\hat{\mathbb{S}}^{-1}\hat{\mathcal{L}}_\#\hat{\mathbb{S}}\, t}|\rho_0\rangle_\#. \end{aligned}\tag{A2}$$

Then we need to verify that $\hat{\mathbb{S}}^{-1}\hat{\mathcal{L}}_\#(+\xi)\hat{\mathbb{S}} = \hat{\mathcal{L}}_\#(-\xi)$ under conditions (i) and (ii). With Eq. (3), we obtain the equation in Fig. 5(d), which further yields

$$\begin{aligned}&\hat{\mathbb{S}}^{-1}\hat{\mathcal{L}}_\#(+\xi)\hat{\mathbb{S}} \\ &\quad= i(\hat{S}^{-1}\hat{H}\hat{S}\otimes\hat{I} - \hat{I}\otimes(\hat{S}^{-1}\hat{H}\hat{S})^T) \\ &\qquad+\sum_\mu\left(\hat{L}_\mu\otimes\hat{L}_\mu^* - \frac{1}{2}\hat{L}_\mu^\dagger\hat{L}_\mu\otimes\hat{I} - \frac{1}{2}\hat{I}\otimes\hat{L}_\mu^T\hat{L}_\mu^*\right),\end{aligned}\tag{A3}$$

where we have used $\hat{S}^{-1}\hat{L}_\mu S = e^{i\phi}\hat{L}_\mu$, $(\hat{S}^T)^{-1} = (\hat{S}^{-1})^T$ as well as the antiunitary relation $\hat{S}^{-1}i\hat{S} = -i$. Furthermore, we have $\hat{S}^{-1}\hat{H}_0\hat{S} = -\hat{H}_0$ and $\hat{S}^{-1}\hat{H}_{\rm int}\hat{S} = \hat{H}_{\rm int}$, which lead to

$$\hat{S}^{-1}\hat{H}(+\xi)\hat{S} = \hat{S}^{-1}(\hat{H}_0 + \xi\hat{H}_{\rm int})\hat{S}, \tag{A4}$$

$$= -\hat{H}_0 + \xi\hat{H}_{\rm int} = -\hat{H}(-\xi). \tag{A5}$$

Thus, Eq. (A3) yields

$$\begin{aligned}&\hat{\mathbb{S}}^{-1}\hat{\mathcal{L}}_\#(+\xi)\hat{\mathbb{S}} \\ &\quad= -i(\hat{H}(-\xi)\otimes\hat{I} - \hat{I}\otimes\hat{H}(-\xi)^T) \\ &\qquad+\sum_\mu\left(\hat{L}_\mu\otimes\hat{L}_\mu^* - \frac{1}{2}\hat{L}_\mu^\dagger\hat{L}_\mu\otimes\hat{I} - \frac{1}{2}\hat{I}\otimes\hat{L}_\mu^T\hat{L}_\mu^*\right) \\ &\quad= \hat{\mathcal{L}}_\#(-\xi)\end{aligned}\tag{A6}$$

Combining Eqs. (A2) and (A6), we obtain the relation $\langle\hat{O}(t)\rangle_{+\xi} = \pm\langle\hat{O}(t)\rangle_{-\xi}$, as expressed in Sec. II.

[1] L. Hackermüller, U. Schneider, M. Moreno-Cardoner, T. Kitagawa, T. Best, S. Will, E. Demler, E. Altman, I. Bloch, and B. Paredes, Science **327**, 1621 (2010).

[2] U. Schneider, L. Hackermüller, J. P. Ronzheimer, S. Will, S. Braun, T. Best, I. Bloch, E. Demler, S. Mandt, D. Rasch, and A. Rosch, Nat. Phys. **8**, 213 (2012).

[3] M. Schreiber, S. S. Hodgman, P. Bordia, H. P. Lüschen, M. H. Fischer, R. Vosk, E. Altman, U. Schneider, and I. Bloch, Science **349**, 842 (2015).

[4] E. J. Meier, F. A. An, and B. Gadway, Nat. Commun. **7**, 1 (2016).

[5] M. E. Tai, A. Lukin, M. Rispoli, R. Schittko, T. Menke, D. Borgnia, P. M. Preiss, F. Grusdt, A. M. Kaufman, and M. Greiner, Nature (London) **546**, 519 (2017).

[6] J. Yu, N. Sun, and H. Zhai, Phys. Rev. Lett. **119**, 225302 (2017).

[7] R. El-Ganainy, K. G. Makris, M. Khajavikhan, Z. H. Musslimani, S. Rotter, and D. N. Christodoulides, Nat. Phys. **14**, 11 (2018).

[8] J. Li, A. K. Harter, J. Liu, L. de Melo, Y. N. Joglekar, and L. Luo, Nat. Commun. **10**, 855 (2019).

[9] S. Yao and Z. Wang, Phys. Rev. Lett. **121**, 086803 (2018).

[10] F. Song, S. Yao, and Z. Wang, Phys. Rev. Lett. **123**, 170401 (2019).

[11] S. Longhi, Phys. Rev. Research **1**, 023013 (2019).

[12] C. Ates, B. Olmos, W. Li, and I. Lesanovsky, Phys. Rev. Lett. **109**, 233003 (2012).

[13] M. Lemeshko and H. Weimer, Nat. Commun. **4**, 2230 (2013).

[14] H. Carmichael, J. Phys. B: At. Mol. Phys. **13**, 3551 (1980).

[15] J. Kasprzak, M. Richard, S. Kundermann, A. Baas, P. Jeambrun, J. M. J. Keeling, F. M. Marchetti, M. H. Szymańska, R. André, J. L. Staehli, V. Savona, P. B. Littlewood, B. Deveaud, and L. S. Dang, Nature (London) **443**, 409 (2006).

[16] A. Amo, D. Sanvitto, F. P. Laussy, D. Ballarini, E. del Valle, M. D. Martin, A. Lemaître, J. Bloch, D. N. Krizhanovskii, M. S. Skolnick, C. Tejedor, and L. Viña, Nature (London) **457**, 291 (2009).

[17] P. Werner, K. Völker, M. Troyer, and S. Chakravarty, Phys. Rev. Lett. **94**, 047201 (2005).

[18] L. Capriotti, A. Cuccoli, A. Fubini, V. Tognetti, and R. Vaia, Phys. Rev. Lett. **94**, 157001 (2005).

[19] M. J. Hartmann, Phys. Rev. Lett. **104**, 113601 (2010).

[20] K. Baumann, C. Guerlin, F. Brennecke, and T. Esslinger, Nature (London) **464**, 1301 (2010).

[21] D. Nagy, G. Kónya, G. Szirmai, and P. Domokos, Phys. Rev. Lett. **104**, 130401 (2010).

[22] S. Diehl, A. Tomadin, A. Micheli, R. Fazio, and P. Zoller, Phys. Rev. Lett. **105**, 015702 (2010).

[23] A. Tomadin, S. Diehl, and P. Zoller, Phys. Rev. A **83**, 013611 (2011).

[24] T. E. Lee, H. Häffner, and M. C. Cross, Phys. Rev. A **84**, 031402(R) (2011).

[25] E. M. Kessler, G. Giedke, A. Imamoglu, S. F. Yelin, M. D. Lukin, and J. I. Cirac, Phys. Rev. A **86**, 012116 (2012).

[26] M. Höning, M. Moos, and M. Fleischhauer, Phys. Rev. A **86**, 013606 (2012).

[27] T. E. Lee, S. Gopalakrishnan, and M. D. Lukin, Phys. Rev. Lett. **110**, 257204 (2013).

[28] Emanuele G. Dalla Torre, S. Diehl, M. D. Lukin, S. Sachdev, and P. Strack, Phys. Rev. A **87**, 023831 (2013).

[29] N. Malossi, M. M. Valado, S. Scotto, P. Huillery, P. Pillet, D. Ciampini, E. Arimondo, and O. Morsch, Phys. Rev. Lett. **113**, 023006 (2014).

[30] M. Marcuzzi, E. Levi, S. Diehl, J. P. Garrahan, and I. Lesanovsky, Phys. Rev. Lett. **113**, 210401 (2014).

[31] N. Lang and H. P. Büchler, Phys. Rev. A **92**, 012128 (2015).

[32] J. Jin, A. Biella, O. Viyuela, L. Mazza, J. Keeling, R. Fazio, and D. Rossini, Phys. Rev. X **6**, 031011 (2016).

[33] S. R. K. Rodriguez, W. Casteels, F. Storme, N. Carlon Zambon, I. Sagnes, L. Le Gratiet, E. Galopin, A. Lemaître, A. Amo, C. Ciuti, and J. Bloch, Phys. Rev. Lett. **118**, 247402 (2017).

[34] R. Rota, F. Storme, N. Bartolo, R. Fazio, and C. Ciuti, Phys. Rev. B **95**, 134431 (2017).

[35] J. Jin, A. Biella, O. Viyuela, C. Ciuti, R. Fazio, and D. Rossini, Phys. Rev. B **98**, 241108(R) (2018).

[36] M.-J. Hwang, P. Rabl, and M. B. Plenio, Phys. Rev. A **97**, 013825 (2018).

[37] R. Rota, F. Minganti, A. Biella, and C. Ciuti, New J. Phys. **20**, 045003 (2018).

[38] D. Huybrechts and M. Wouters, Phys. Rev. A **99**, 043841 (2019).

[39] S. Diehl, A. Micheli, A. Kantian, B. Kraus, H. Büchler, and P. Zoller, Nat. Phys. **4**, 878 (2008).

[40] M. Müller, S. Diehl, G. Pupillo, and P. Zoller, Adv. At. Mol. Opt. Phys. **61**, 1 (2012).

[41] B. T. Torosov, G. Della Valle, and S. Longhi, Phys. Rev. A **87**, 052502 (2013).

[42] A. J. Daley, Adv. Phys. **63**, 77 (2014).

[43] J. Otterbach and M. Lemeshko, Phys. Rev. Lett. **113**, 070401 (2014).

[44] C. Yang, D. Li, and X. Shao, Sci. China: Phys. Mech. Astron. **62**, 110312 (2019).

[45] K. V. Kepesidis and M. J. Hartmann, Phys. Rev. A **85**, 063620 (2012).

[46] A. Le Boité, G. Orso, and C. Ciuti, Phys. Rev. Lett. **110**, 233601 (2013).

[47] G. Kordas, D. Witthaut, P. Buonsante, A. Vezzani, R. Burioni, A. Karanikas, and S. Wimberger, Eur. Phys. J.: Spec. Top. **224**, 2127 (2015).

[48] J. T. Barreiro, M. Müller, P. Schindler, D. Nigg, T. Monz, M. Chwalla, M. Hennrich, C. F. Roos, P. Zoller, and R. Blatt, Nature (London) **470**, 486 (2011).

[49] R. Blatt and C. F. Roos, Nat. Phys. **8**, 277 (2012).

[50] J. G. Bohnet, B. C. Sawyer, J. W. Britton, M. L. Wall, A. M. Rey, M. Foss-Feig, and J. J. Bollinger, Science **352**, 1297 (2016).

[51] H. Deng, H. Haug, and Y. Yamamoto, Rev. Mod. Phys. **82**, 1489 (2010).

[52] A. Tomadin, V. Giovannetti, R. Fazio, D. Gerace, I. Carusotto, H. E. Türeci, and A. Imamoglu, Phys. Rev. A **81**, 061801(R) (2010).

[53] T. C. H. Liew and V. Savona, New J. Phys. **15**, 025015 (2013).

[54] M. Fitzpatrick, N. M. Sundaresan, A. C. Y. Li, J. Koch, and A. A. Houck, Phys. Rev. X **7**, 011016 (2017).

[55] G. Lindblad, Commun. Math. Phys. **48**, 119 (1976).

[56] P. Pearle, Eur. J. Phys. **33**, 805 (2012).

[57] C. A. Brasil, F. F. Fanchini, and R. d. J. Napolitano, Rev. Bras. Ensino Fis. **35**, 01 (2013).

[58] V. V. Albert and L. Jiang, Phys. Rev. A **89**, 022118 (2014).

[59] F. Minganti, A. Biella, N. Bartolo, and C. Ciuti, Phys. Rev. A **98**, 042118 (2018).
[60] D. Nigro, J. Stat. Mech. (2019) 043202.
[61] M. Zwolak and G. Vidal, Phys. Rev. Lett. **93**, 207205 (2004).
[62] A. Kshetrimayum, H. Weimer, and R. Orús, Nat. Commun. **8**, 1291 (2017).
[63] H. P. Büchler, A. Micheli, and P. Zoller, Nat. Phys. **3**, 726 (2007).
[64] P. R. Johnson, E. Tiesinga, J. V. Porto, and C. J. Williams, New J. Phys. **11**, 093022 (2009).
[65] S. Ejima, F. Lange, H. Fehske, F. Gebhard, and K. zu Münster, Phys. Rev. A **88**, 063625 (2013).
[66] S. Paul, P. R. Johnson, and E. Tiesinga, Phys. Rev. A **93**, 043616 (2016).
[67] E. G. C. P. van Loon, M. I. Katsnelson, and M. Lemeshko, Phys. Rev. B **92**, 081106(R) (2015).
[68] S. Baier, M. J. Mark, D. Petter, K. Aikawa, L. Chomaz, Z. Cai, M. Baranov, P. Zoller, and F. Ferlaino, Science **352**, 201 (2016).
[69] A. Mazurenko, C. S. Chiu, G. Ji, M. F. Parsons, M. Kanász-Nagy, R. Schmidt, F. Grusdt, E. Demler, D. Greif, and M. Greiner, Nature (London) **545**, 462 (2017).
[70] H. Weimer, Phys. Rev. A **91**, 063401 (2015).
[71] J. Cui, J. I. Cirac, and M. C. Bañuls, Phys. Rev. Lett. **114**, 220601 (2015).
[72] A. H. Werner, D. Jaschke, P. Silvi, M. Kliesch, T. Calarco, J. Eisert, and S. Montangero, Phys. Rev. Lett. **116**, 237201 (2016).
[73] A. A. Gangat, T. I, and Y.-J. Kao, Phys. Rev. Lett. **119**, 010501 (2017).
[74] F. Verstraete, V. Murg, and J. I. Cirac, Adv. Phys. **57**, 143 (2008).
[75] R. Orús, Ann. Phys. **349**, 117 (2014).
[76] Z.-Y. Xie, J. Chen, J. F. Yu, X. Kong, B. Normand, and T. Xiang, Phys. Rev. X **4**, 011025 (2014).
[77] G. Vidal, Phys. Rev. Lett. **98**, 070201 (2007).
[78] H.-C. Jiang, Z.-Y. Weng, and T. Xiang, Phys. Rev. Lett. **101**, 090603 (2008).
[79] R. Orús and G. Vidal, Phys. Rev. B **80**, 094403 (2009).
[80] C. Carr, R. Ritter, C. G. Wade, C. S. Adams, and K. J. Weatherill, Phys. Rev. Lett. **111**, 113901 (2013).
[81] M. F. Maghrebi and A. V. Gorshkov, Phys. Rev. B **93**, 014307 (2016).
[82] V. R. Overbeck, M. F. Maghrebi, A. V. Gorshkov, and H. Weimer, Phys. Rev. A **95**, 042133 (2017).
[83] T. Tomita, S. Nakajima, I. Danshita, Y. Takasu, and Y. Takahashi, Sci. Adv. **3**, e1701513 (2017).
[84] M. A. Nichols, L. Cheuk, M. Okan, T. Hartke, E. Mendez, T. Senthil, E. Khatami, H. Zhang, and M. Zwierlein, Science **363**, 383 (2019).
[85] P. T. Brown, D. Mitra, E. Guardado-Sanchez, R. Nourafkan, A. Reymbaut, C.-D. Hébert, S. Bergeron, A.-M. S. Tremblay, J. Kokalj, D. A. Huse, P. Schauß, and W. S. Bakr, Science **363**, 379 (2019).
[86] H. Zhai, N. Sun, J. Yu, and P. Zhang, New J. Phys. **21**, 015003 (2019).
[87] H. Pichler, A. J. Daley, and P. Zoller, Phys. Rev. A **82**, 063605 (2010).
[88] H. P. Breuer, E. M. Laine, J. Piilo, and B. Vacchini, Rev. Mod. Phys. **88**, 021002 (2016).
[89] I. de Vega and D. Alonso, Rev. Mod. Phys. **89**, 015001 (2017).
[90] H.-P. Breuer, Phys. Rev. A **70**, 012106 (2004).
[91] J. Piilo, S. Maniscalco, K. Harkonen, and K. A. Suominen, Phys. Rev. Lett. **100**, 180402 (2008).